Ytterbium disilicate-based glass-ceramic as joining material for ceramic matrix composites

Ytterbium disilicate-based glass-ceramic as joining material for ceramic matrix composites

Federico Smeacetto[1]*, Fabiana D'Isanto[1], Valentina Casalegno[1], Peter Tatarko[2], Milena Salvo[1]

[1]*Department of Applied Science and Technology, DISAT, Politecnico di Torino, Corso Duca degli Abruzzi 24, 10129 Torino, Italy*

[2] *Institute of Inorganic Chemistry Slovak Academy of Sciences Dubravska cesta 9 845 36 Bratislava Slovakia*

* Corresponding author: *E-mail: federico.smeacetto@polito.it*
Tel:+39 011 0904756; fax: Tel:+39 011 0904699

Keywords: joining, glass, ceramic matrix composites

Abstract: A key aspect of ceramic matrix composites integration is related to a reliable joining technique. An ytterbium disilicate based glass-ceramic material is processed by reactive viscous flow sintering between a barium aluminium borosilicate glass and ytterbium oxide and it is used to join SiC/SiC and C/SiC composites. The joining temperature and the in situ formation of the $Yb_2Si_2O_7$ is optimised at 1200°C without pressure, on the basis of the sintering and crystallisation mechanisms. The mechanical characterization of SiC/SiC and C/SiC joined with the ytterbium disilicate-based glass-ceramic, tested by single-lap offset at RT, exhibits an apparent shear strength of 35 MPa, similar to their interlaminar shear strength.

The proposed system displays self-healing behaviour at 1000°C and 1150°C, as demonstrated by the partial and complete sealing of induced cracks by Vickers indentation on its surface at different loads, thus suggesting that it can effectively be used as promising joining material for CMCs.

1. Introduction

Ceramic matrix composites (CMCs) are considered the most appropriate candidates to progressively replace metallic alloys in a wide range of applications thanks to their excellent thermomechanical properties coupled with a low density. Since their processing as large components with complex shapes is extremely problematic and expensive, most of the future applications of CMCs depend on their capability to be joined.

The joining of CMC components is one of the toughest challenges facing the application of these composites in high-temperature environments since they cannot be welded by conventional methods and the use of ceramic rivets and bolts is not sufficient to produce a gas tight joining [1,2].

Different techniques for the joining of CMCs materials have been proposed, including solid-state diffusion [3], laser-supported joining [4], transient liquid-phase joining, metallic brazing and preceramic polymer-to-ceramic conversion [5–7]. A considerable amount of literature has been published on these specific methods, highlighting different temperatures, pressures, and joining materials as the main factors to be considered for joining SiC-based materials [8-10].

Glasses and glass-ceramics are considered very good candidates to join CMCs to themselves and to other materials. Due to their high viscous flow, these materials can successfully be used as joining materials for CMCs. The “glass-ceramic route” can be used as a pressure less method for high temperature applications. Glass-ceramics can be processed through sintering and crystallization of powdered glasses. It is possible to process advanced glass-ceramic materials with exceptional features thanks to the great flexibility of parent glass compositions and the versatile sinter-crystallization method. Furthermore, joining monolithic SiC or SiC-based composites with a glass-ceramic can offer several advantages, including hermeticity, possible self-healing by viscous flow of the residual glassy phase at medium-high temperatures, tailorable coefficient of thermal expansion (CTE) and the possibility to avoid the use of pressure.

Recently $Yb_2Si_2O_7$ gained a lot of interest [11] and it is currently one of the most promising ceramic materials for environmental barriers coatings, usually processed by plasma spray techniques.

However, it is quite challenging to fabricate a layer of pure $Yb_2Si_2O_7$ layer since Yb_2SiO_5 co-exists with the $Yb_2Si_2O_7$ in the coating. This is due to the segregation of Yb_2SiO_5 from the SiO_2-depleted $Yb_2Si_2O_7$ regions during the deposition [12]. $Yb_2Si_2O_7$ has a CTE of 4.1 x 10^{-6} K^{-1} [13], very close to the SiC and SiC/SiC ones, thus suggesting its use as a joining material for SiC-based CMCs.

An interesting approach is to produce in situ the desired $Yb_2Si_2O_7$ phase by a reactive viscous sintering approach. Even if there is a growing body of literature that recognises the importance of glass-ceramics as joining materials, few papers deal with the possibility of using a specific glass composition as a matrix in which is possible to grow in situ specific crystalline phases with desired properties by reactive viscous flow sintering [14].

The specific objective of this study is to join C/SiC and SiC/SiC substrates with an ytterbium disilicate based glass-ceramic, in situ processed by reactive viscous flow sintering between a barium aluminium borosilicate glass matrix and ytterbium oxide.

2. Experimental

SiC/SiC Keraman® (SiC Tyranno Type S, crystalline CVI SiC matrix; a pyrolitic carbon fiber/matrix interface, MT Aerospace, now BJS composites, Germany) with a CTE of 4.0 x 10^{-6} K^{-1} and C/SiC Keraman® (CVI, MT Aerospace, now BJS composites, Germany) with CTE = // 2.0 x 10^{-6} K^{-1}; ⊥ 4.0 x 10^{-6} K^{-1}) were used as substrates.

The glass matrix used in this work (referred to as SABB) was produced by conventional melting and casting method and has the following composition 70.4 SiO_2, 2.1 Al_2O_3, 17.5 B_2O_3, 10 BaO; details on this borosilicate glass are reported in [15]. Ytterbium oxide powders <38 µm were obtained from 3- 12 mm sintered lump (99.9% purity, Alfa Aesar) with ball milling and sieving.

For the glass synthesis, different precursor powders were thoroughly mixed for 24h and subsequently melted at 1650-1700°C for five hours in a Rh-Pt crucible. The molten glass was then quenched on a brass plate followed by ball milling and sieving to obtain glass particles <38 µm. The sintering behaviour was analyzed by means of a heating stage microscope (HSM, Hesse Instruments,

Harzgerode Germany) at a heating rate of 10°C/min. Glass matrix and Yb_2O_3 powders were mixed (2:1 by weight), uniaxially pressed and sintered at 1200°C for 1 hour in order to obtain glass-ceramic sintered discs. The X-ray diffraction analysis was carried out on as-sintered samples, between 10° and 70° using a X'Pert Pro MRD diffractometer with Cu Kα radiation (PANalytical X'Pert Pro, Philips, Almelo, The Netherlands), with the aid of the X-Pert HighScore software; the phases were identified using JCPDS database provided by ICDD (International Centre for Diffraction Data, Newton Square, Pennsylvania, USA).

The coefficient of thermal expansion (CTE) of as-sintered glass-ceramic was measured by means of a dilatometer (Netzsch, DIL 402 PC/4).

A slurry made of a mixture of SABB glass and Yb_2O_3 particles (2:1 by weight), dispersed in ethanol (1:2 weight ratio), was manually deposited between C/SiC and SiC/SiC substrates. The joining process was carried out in a tubular furnace (STF 16/ 180, Carbolite Gero, Hope Valley, UK) under a continuous Ar flowing, at 1200°C, for 1 hour.

A field emission scanning electron microscope (FE-SEM, Merlin electron microscope, ZEISS, Oberkochen, Germany) with energy dispersive X-ray spectroscopy (EDS, Zeiss Supra TM 40, Oberkochen, Germany) was used to characterise the morphology of the samples, which were previously polished using SiC papers (grit size 600-4000) and coated with Cr. A benchtop scanning electron microscope (SEM, JCM-6000 plus, Jeol, Peabody, Massachusetts, USA) was used to observe the fracture surfaces of the samples after the mechanical tests.

The apparent shear strength of the joined samples was evaluated using the single lap offset (SLO) test under compression at room temperature, according to a method adapted from ASTMD905-08 [16] (universal testing machine SINTEC D/10); the crosshead speed was 0.5 mm/min. The apparent shear strength was calculated dividing the maximum force by the joining area. The size of the single lap off-set shear tests for brazed samples was about 12.5 mm × 4 mm × 3 mm with different joined areas (at least 3 samples for each joint).

In order to observe potential crack healing behaviour of the glass-ceramic matrix, a series of Vickers indents at various loads (0.5 and 1 kg) were placed into the surface of the samples (Zwick/Roell ZHU/Z2.5, Germany). At least 5 indents were introduced at each indentation load. The thermal treatment of the sample was then carried out in a furnace (Netzsch-Gerätebau GmbH, Germany) at temperatures of 1000°C and 1150°C in air with the dwell time of 30 and 20 minutes, respectively. The heating and cooling rates were 15°C/min. The depth of the indents was measured using a confocal microscope (Olympus LEXT OLS3100, Japan). The indents before and after thermal treatment were also observed using an optical microscope (VHX-1000 Keyence, USA).

3. Results and Discussion

Figure 1a shows the experimental data obtained from hot stage microscopy experiments on the SABB glass matrix and a mixture of glass matrix and ytterbia particles (2:1 by weight), where the linear shrinkages are plotted against the temperature. The most interesting aspect of this graph is that while the first shrinkage temperature (T_{fs}), which is determined by the glass matrix, is only slightly affected by the presence of ytterbia particles, a different behaviour was observed after that sintering started. Interestingly, there were differences in the characteristic fixed viscosity points of the two systems, such as deformation temperature (T_D), sphere temperature (T_{sp}) and half sphere (T_{hs}), as well as in the trend of the curves. The curve of the glass matrix exhibited a progressive shrinkage, typical behaviour of a viscous flow of the glass; the system composed of glass matrix and ytterbia particles displayed both a delay in terms of deformation temperature as well as the presence of a plateau between 1100 and 1400°C. This result may be explained by the fact that an increase of viscosity is due to the addition of ytterbia particles, but the most remarkable observation to emerge from the data comparison was that the freezing of shrinkage at 1100°C could be likely due to a crystallisation phenomenon, which hinders further shrinkage by viscous flow.

Figure 1b shows a trend line to predict the viscosity of the system vs temperature, obtained by plotting the characteristic temperatures at fixed viscosity values shown in Table I.

On the basis of these analyses, the thermal treatment to process sintered pellets to obtain the glass-ceramic system was chosen at 1200°C for 1 hour, since a value of viscosity around 10^6 Pa·s is obtained; this value is considered suitable to allow a good glass flow, wetting and bonding of the CMC substrates.

The glass matrix used in this study has a CTE of 1.8 x10^{-6} K^{-1} (300–600 °C) [17]; the addition of Yb_2O_3 particles, followed by a heat treatment at 1200°C, with 1h dwelling, led to the formation of a glass-ceramic with a CTE of 3.4 x 10^{-6} K^{-1} (RT-500°C), as deduced by dilatometer measurements (not reported here).

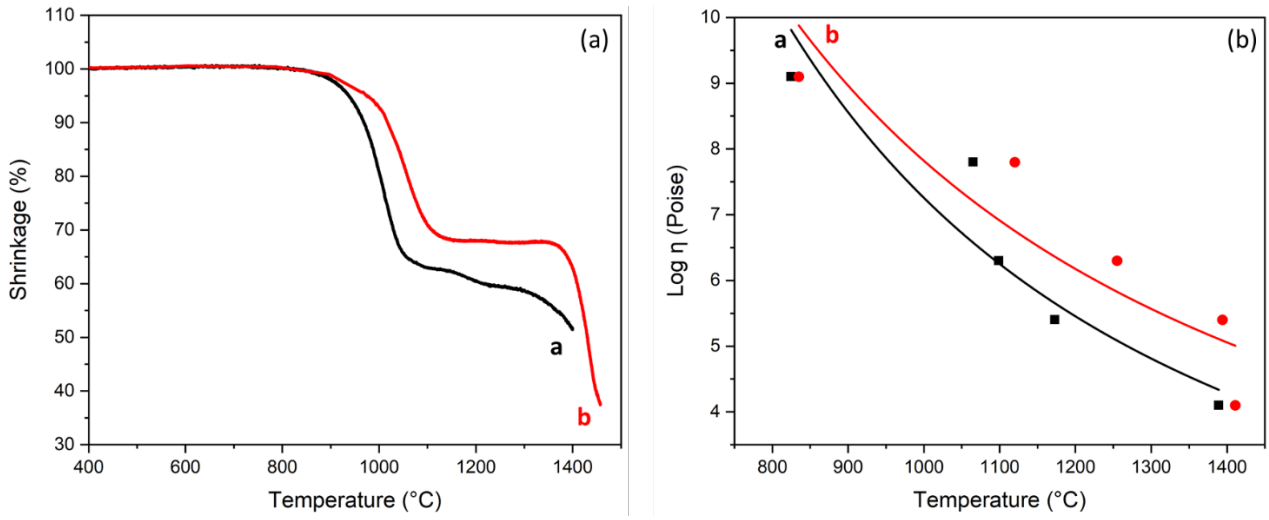

Figure 1. (a) Hot stage microscope analyses of the SABB glass (curve a) and SABB+Yb_2O_3 mixture 2:1 wt. (curve b), both recorded at 10 °C/min. (b) Log η vs Temperature curve for the SABB glass (curve a) and SABB+Yb_2O_3 mixture (2:1 by weight) (curve b), obtained by fitting the characteristic fixed viscosity points and related temperatures (T_{fs}, T_{ms}, T_D, T_{sp}, T_{hs}) reported in Table I.

Table I. Characteristic temperatures at fixed viscosity values for the SABB glass and the SABB+Yb_2O_3 mixture (2:1 by weight). Viscosity values from [18].

	SABB glass T (°C)	**SABB + Yb_2O_3 (2:1 wt) mixture T (° C)**	**Log η (Poise)**
T_{fs}	825	835	9.1
T_{ms}	1065	1120	7.8
T_D	1099	1255	6.3
T_{sp}	1173	1394	5.4
T_{hs}	1389	1411	4.1

Figure 2 shows the XRD pattern of the SABB glass and ytterbia powders mixture (2:1 by weight) after the heat treatment at 1200°C for 1 hour. Yb disilicate was detected as the main crystalline phase, together with the presence of a small amount of ytterbia and a residual amorphous phase. The presence of a tiny residual ytterbia phase might suggest that the reaction does not propagate homogenously throughout the total volume of the powder.

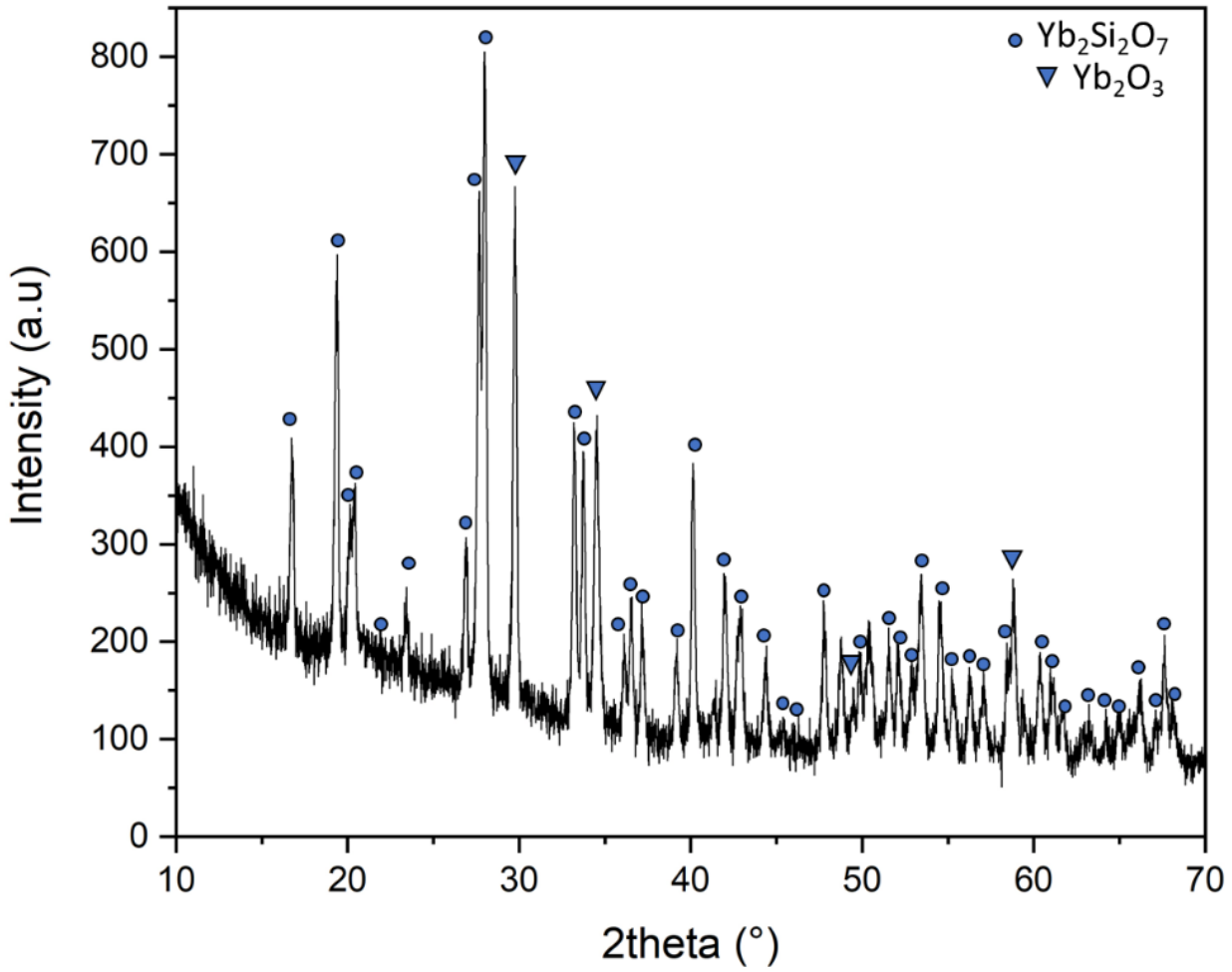

Figure 2. XRD pattern of the mixture of SABB glass and ytterbia mixture (2:1 by weight) after the heat treatment at 1200°C for 1 hour; $Yb_2Si_2O_7$ indexed by the PDF card n. 00-025-1345; Yb_2O_3 indexed by the PDF card n. 01-074-1981.

SiC/SiC and C/SiC joined samples were processed on the basis of previous findings and considerations on viscosity, shrinkage behaviour and new crystalline phase formation.

As it can be seen in Figure 3, the SEM on a cross-sectioned joined CMCs showed excellent adhesion of ytterbium disilicate based glass-ceramic with both SiC/SiC and C/SiC composites. No defects were located at the interface (Figure 3 b and d), where a strong connection between the ytterbium disilicate based glass-ceramic and the composites substrates was observed; an average joint thickness of 450 µm was obtained without using any pressure, but only taking advantage of the viscous flowing behaviour of the proposed system.

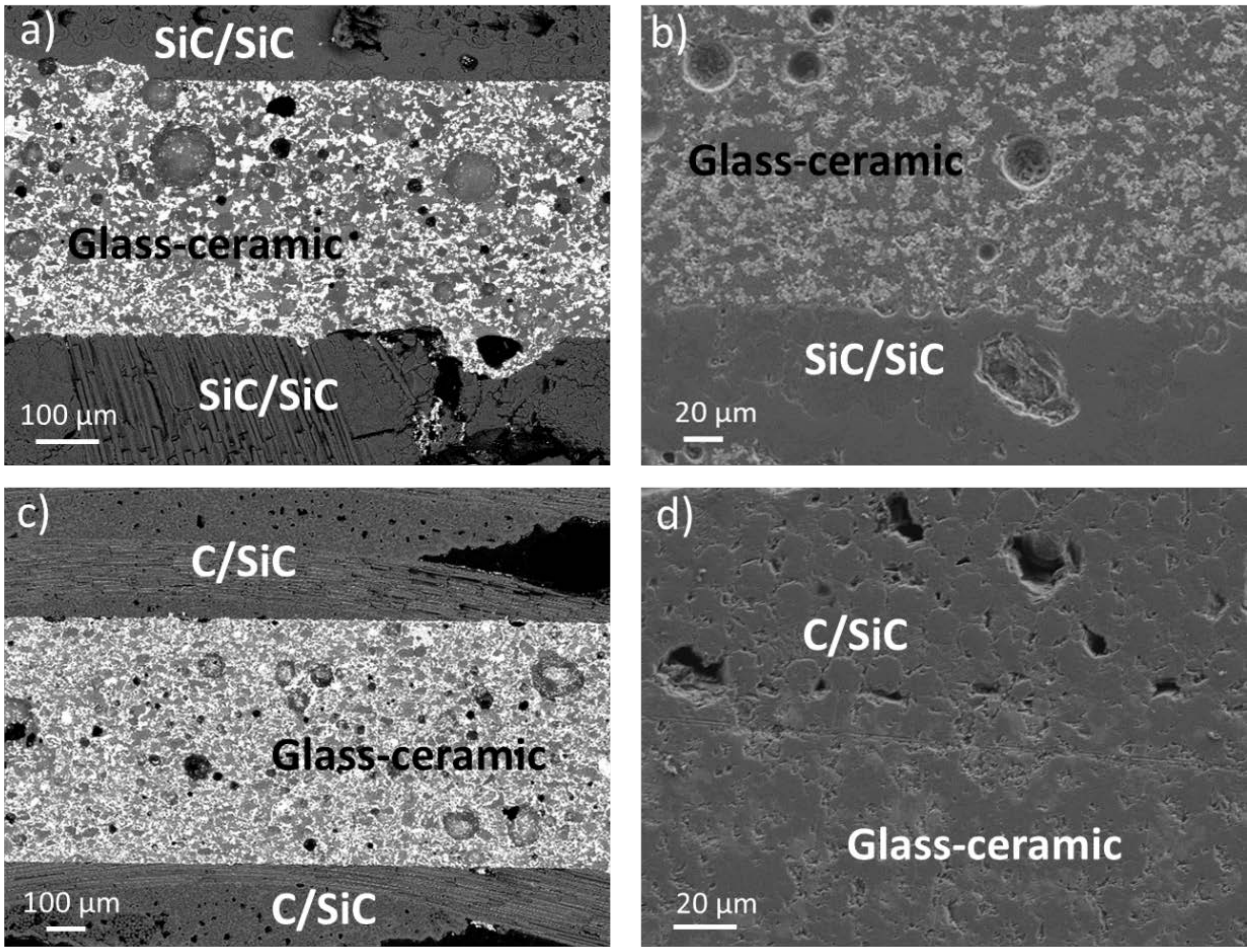

Figure 3. SEM images of the cross-section of (a, b) a glass-ceramic joined SiC/SiC sample and (c,d) a glass-ceramic joined C/SiC sample.

The presence of a few closed porosities is determined by the manual slurry method used to obtain the joined samples, thus suggesting that a different joining technology should be foreseen. Furthermore, no evident reaction took place at the interface between the glass-ceramic and the composites. As detected by XRD measurement, a slight amount of residual ytterbia is present in the glass-ceramic joining system; ytterbium oxide has a CTE of 8.5 ± 0.6 X 10^{-6} K^{-1} [19] and its presence is not detrimental in terms of thermo-mechanical compatibility with the SiC/SiC and C/SiC substrates since, as mentioned above, the CTE of the joining material is similar to the CMCs' ones and no cracks due to thermal residual stresses were observed within the glass-ceramic.

The joined area showed a heterogeneous microstructure in terms of element and phase distribution. This result may be explained by the fact that the ytterbium disilicate phase, formed by reactive viscous

flow sintering between the barium aluminium borosilicate glass matrix and ytterbium oxide, is surrounded and embedded in two different glass phases. In order to have a clear picture, a magnification of the ytterbium disilicate based glass-ceramic taken from the middle of the joining area is shown in figure 4.

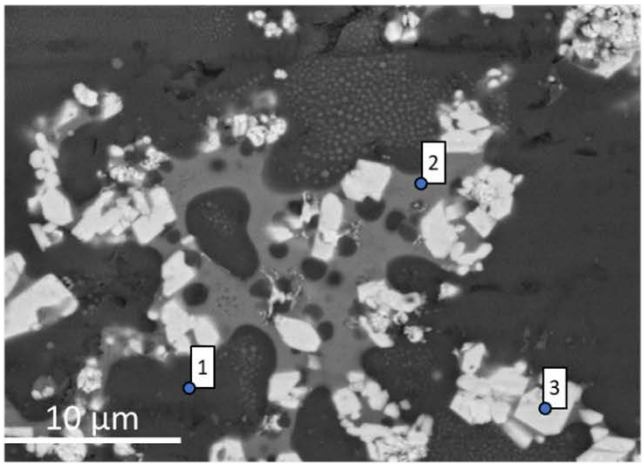

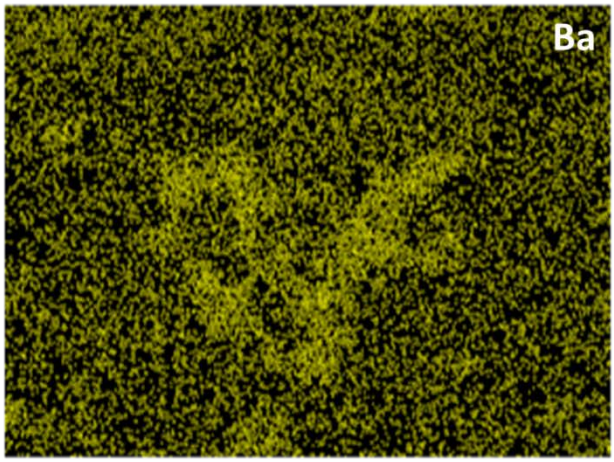

Elements	Spectrum 1 (at%)	Spectrum 2 (at%)	Spectrum 3 (at%)
O	70.9	71.6	65.7
Al	0.8	2.2	-
Si	27.0	19.9	17.9
Ba	1.0	4.8	-
Yb	0.3	1.5	16.4
Total	100.0	100.0	100.0

Figure 4. SEM, Ba elemental map and EDS analyses of the ytterbium disilicate based glass-ceramic from the joining area

The EDS analyses revealed clusters/agglomeration of YbSi2O7 white crystals (spectrum 3) dispersed in the silica-rich glassy phase (spectrum 1); however, an interesting aspect of the SEM-EDS data is that a further matrix is visible and seem to surround and connect the $Yb_2Si_2O_7$ white crystals. This matrix was found to be rich in BaO (spectrum 2), and it is well evident in the elemental distribution map in figure 4. This result may be explained by the fact that, during the viscous sintering at 1200°C, the reaction between silica from the parent glass and Yb_2O_3 particles led to a localised silica depletion

in the original glass matrix. It can, therefore, be assumed that the glass matrix which surrounds the $Yb_2Si_2O_7$ possesses lower characteristic temperatures, due to a lower silica and higher BaO content, with respect to the silica-rich glassy phase. These findings suggest that a beneficial effect in terms of self-healing properties might be effective at intermediate temperatures. A schematic of the whole glass-ceramic system, as described above, is reported in Figure 5 (a, b, c). It can thus be suggested that in case of crack formation (i.e. during cooling of the system or mechanical stress), upon reheating, the BaO rich glassy phase (with a lower softening temperature) could act as a partial or total crack healer.

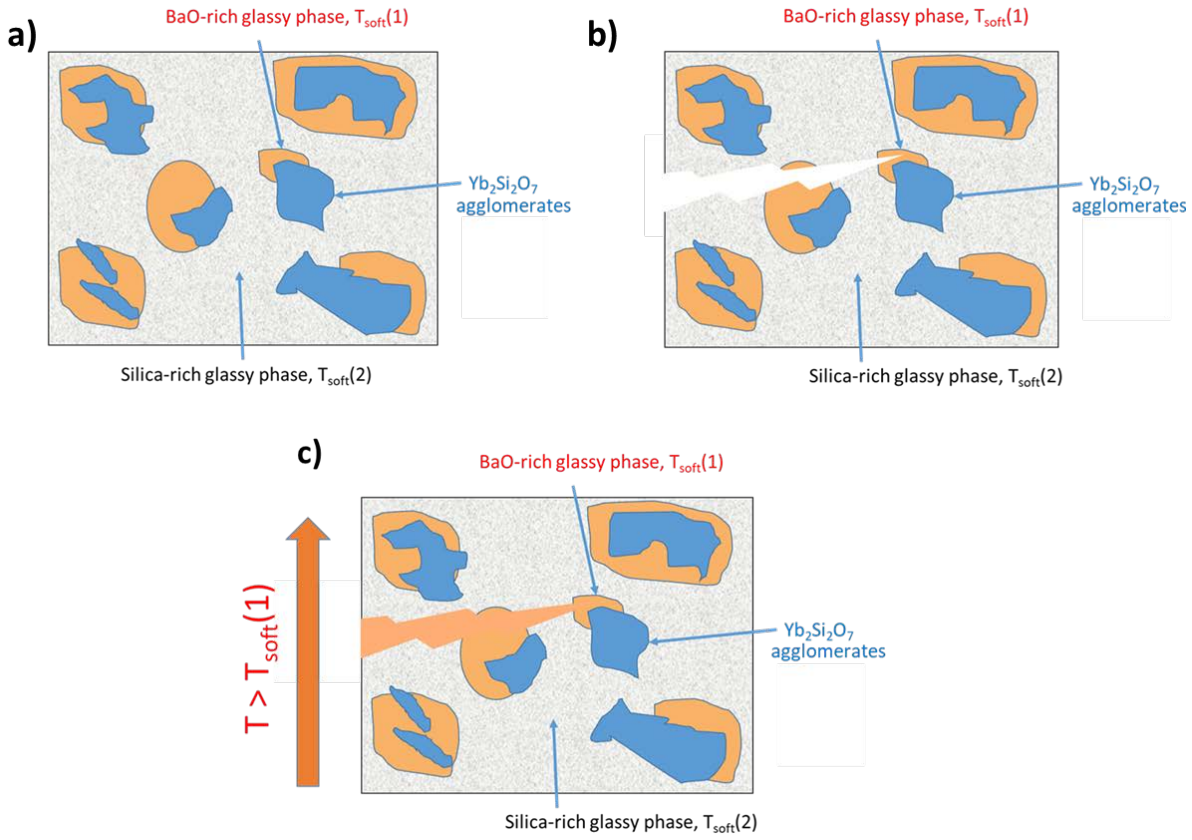

Figure 5. Schematic of the glass-ceramic system microstructure: (a) before and (b) after crack formation, (c) self- healing during reheating at a temperature higher than the softening temperature (T soft) of the Ba-rich glassy phase and lower than the deformation temperature (DT) of the whole glass-ceramic system.

In order to support this hypothesis, Vickers indentations at different loads were introduced onto the polished surface of the joined area. Figure 6 shows the optical images of the Vickers indents made at different loads (HV0.5, HV1) before and after both annealings at 1000°C for 30 min and 1150°C for

20 min. These results show that the indents almost completely vanished after the first heat treatment at 1000°C, while some remaining indentation cracks could still be observed (Figures 6b and 6e) [20]. Both the indents and the indentation cracks completely vanished after the second annealing at 1150°C (Figures 6c and 6f).

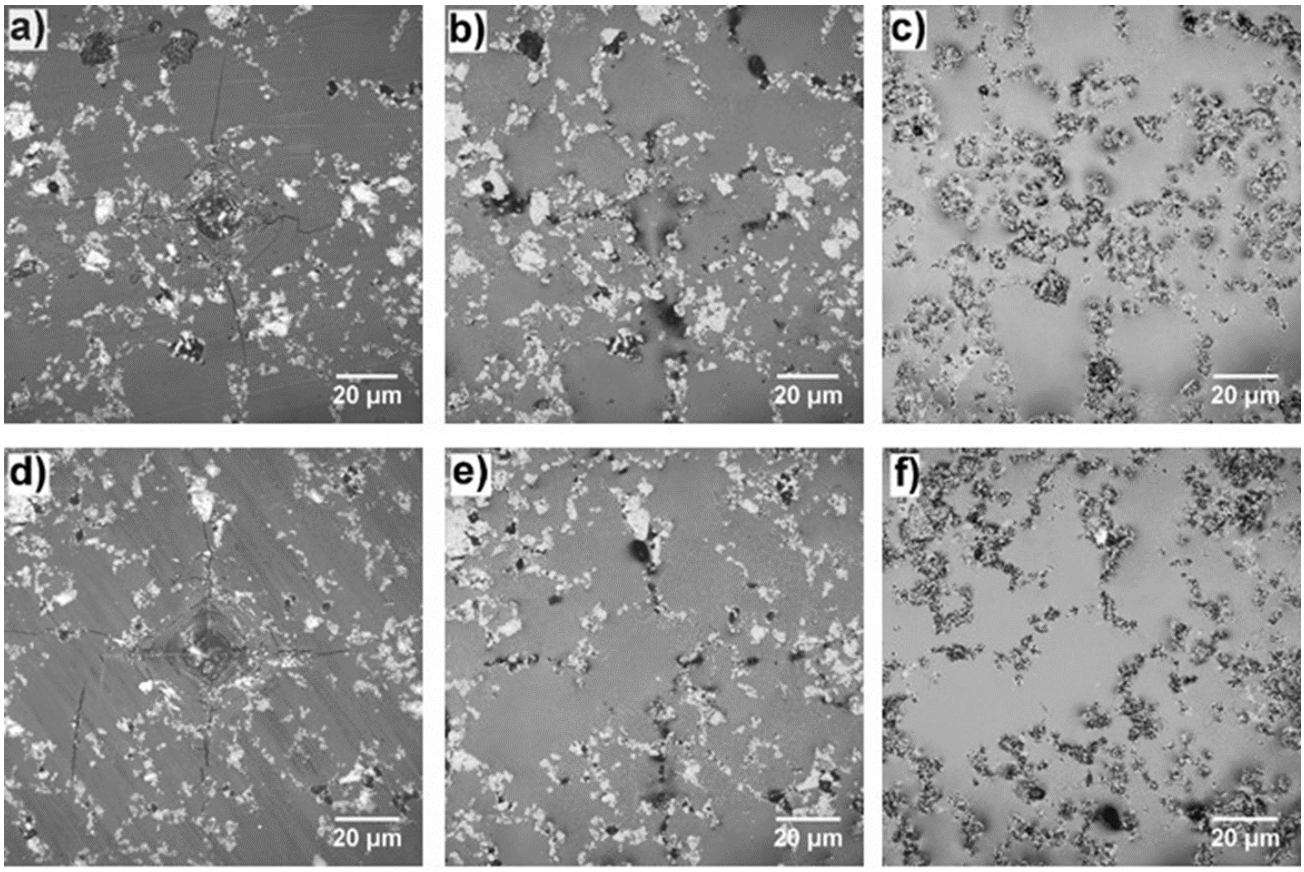

Figure 6. Optical images of the indents made at 0.5 kg (HV0.5) (a) before, (b) after annealing at 1000°C/30 min, and (c) after annealing at 1150°C/20min; 1 kg (HV1) (d) before, (e) after annealing at 1000°C/30 min, and (f) after annealing at 1150°C/20min.

The healing behaviour of a glass-ceramic system was further investigated by measuring the depth of the indents before and after thermal treatment using a confocal microscope. Figure 7 shows the corresponding 3D images of the indents made at 1 kg (HV1) before and after annealing at 1000°C/30 min and 1150°C/20 min, respectively. The depth profile of all indents is given in the inset images on the bottom left corner. It is obvious that the maximum depth of the indents made at 1 kg decreased from 6.5 µm to 3.2 µm after the first treatment at 1000°C (Figures 6a and 6b). Since the second annealing cycle at 1150°C resulted in a complete healing of the indents and the cracks, the depth

profile corresponds to the surface roughness of the samples rather than to the maximum depth of the remaining indent. These results further support the idea that a glass-ceramic system with two different glassy phases shows self-healing behaviour at a temperature lower than the deformation temperature of the whole glass-ceramic (Figure 1 and Table I) but higher than that of the Ba-rich glassy phase, and both the indents and corresponding indentation cracks introduced into the material at loads below 1 kg can be healed by the proposed two-step annealing process.

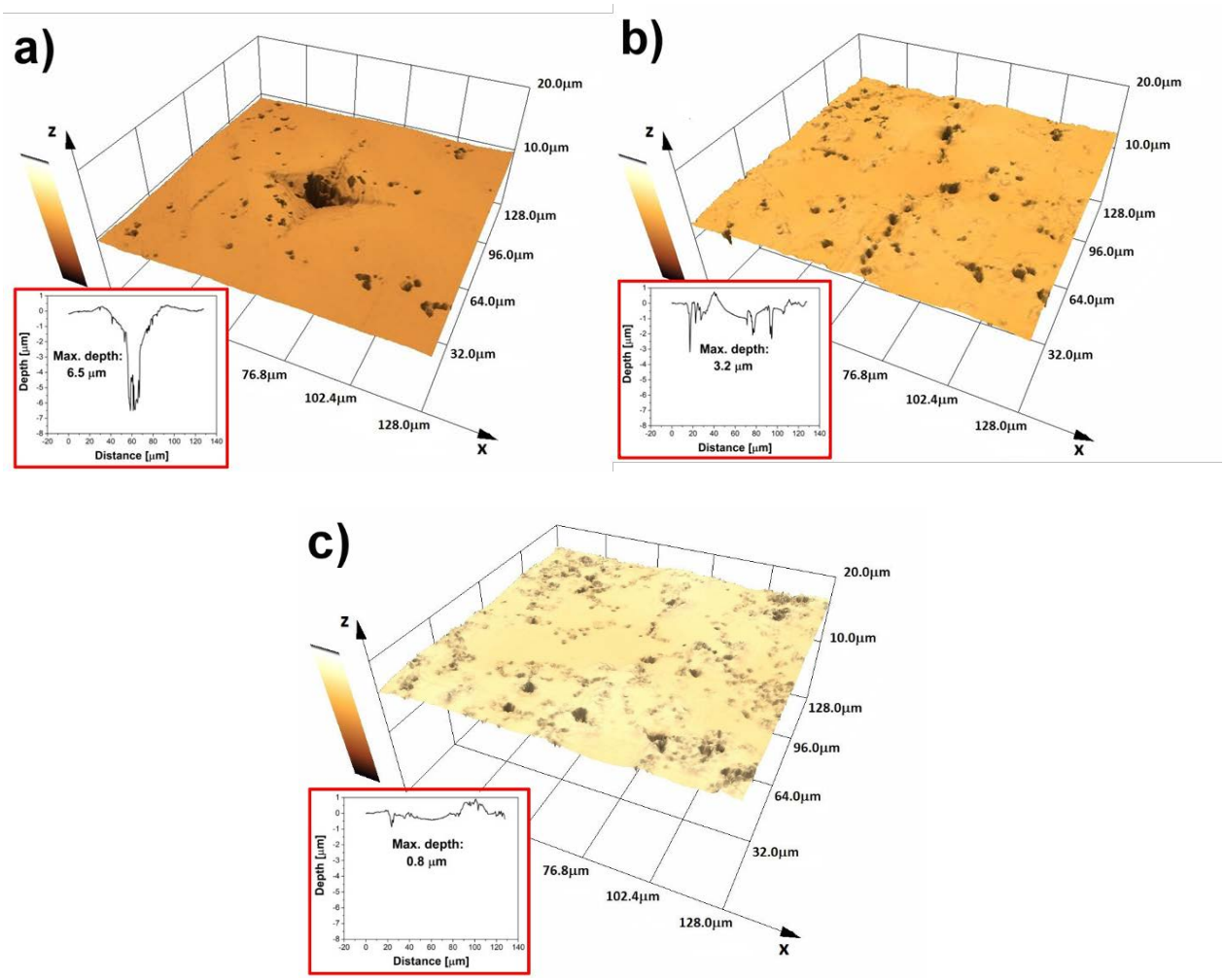

Figure 7. 3D images (confocal microscopy) of the indents made at 1 kg (HV1) (a) before, (b) after annealing at 1000°C/30 min, and (c) after annealing at 1150°C/20 min.

The single lap offset (SLO) test, under compression, was used to evaluate the mechanical properties of the glass-ceramic joined CMCs. The tests carried out on SiC/SiC joints with a joined area of about 42 and 30 mm^2 did not lead to a failure in the joining area and cracks propagated within the composite (Figure 8a). By decreasing the joining area to 20 mm^2 a failure in the joining area, with partial delamination/failure of SiC/SiC was observed and the measured shear strength of the SiC/SiC joint resulted to be 34.7 ± 8.7 MPa (Figure 8b). Figures 8 c, d show a magnification of the fracture surfaces where it is clearly visible the propagation of the failure within the composite.

The mechanical tests on C/SiC joined samples (joining area ~ 35 mm^2) showed a failure in the joining area with an apparent shear strength of 34.8 ± 2.6 MPa. The macrograph of the fracture surfaces is shown in Figure 9a; a closer inspection of the fracture surfaces of the joints (Figure 9 b and c) provided further information about the bonding and adhesion mechanism between the ytterbium disilicate glass ceramic and the SiC based composites and showed that fracture propagated at the glass-ceramic/composite interface and within the glass-ceramic and that the joining material homogeneously adhered on both parts of the C/SiC substrate.

In conclusion, both the SiC/SiC and the C/SiC composites joined with the new ytterbium silicate-based glass-ceramic showed a shear strength of ~35 MPa, which is comparable to the interlaminar shear strength of the CMCs (30-40 MPa).

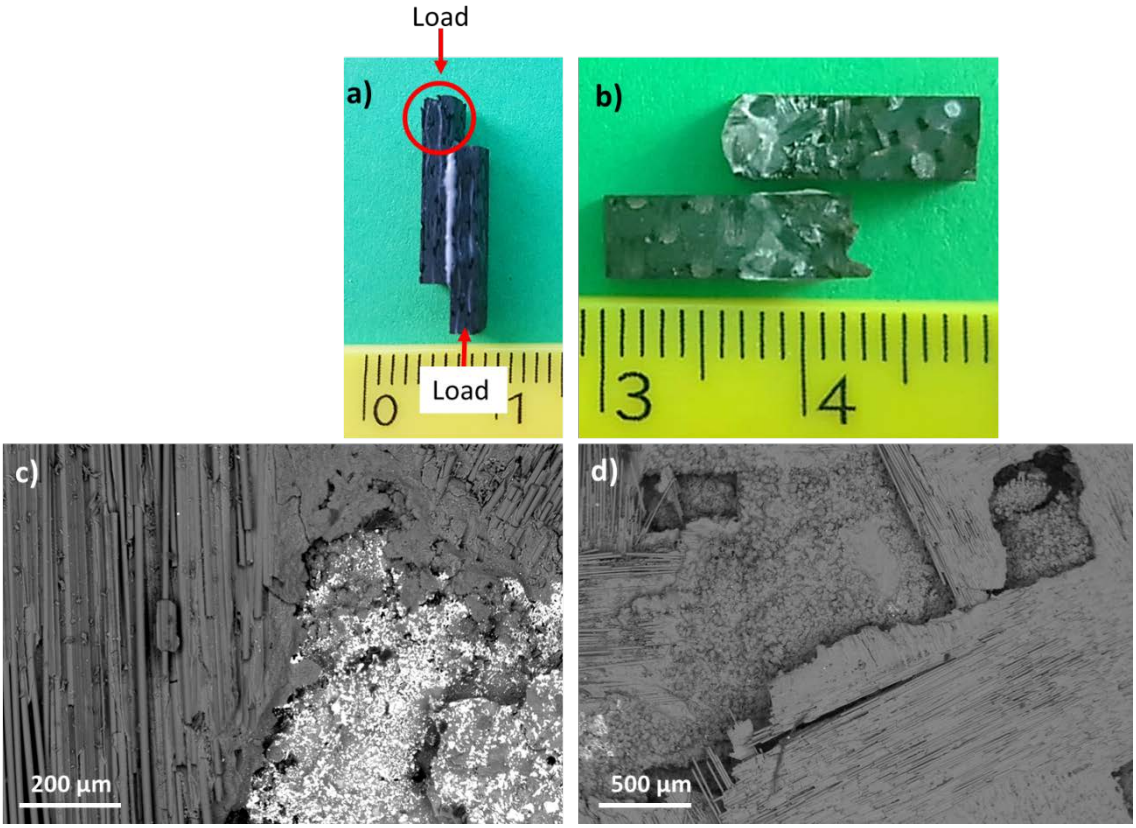

Figure 8. (a, b) Macrographs of a glass-ceramic joined SiC/SiC with a joining area of ~ 42 mm^2 (the red circle indicates the crack formation in the composite) and (c, d) SEM micrographs (BSE) of the fracture surfaces after the SLO mechanical test on a glass-ceramic joined SiC/SiC with a joining area ~ 20 mm^2

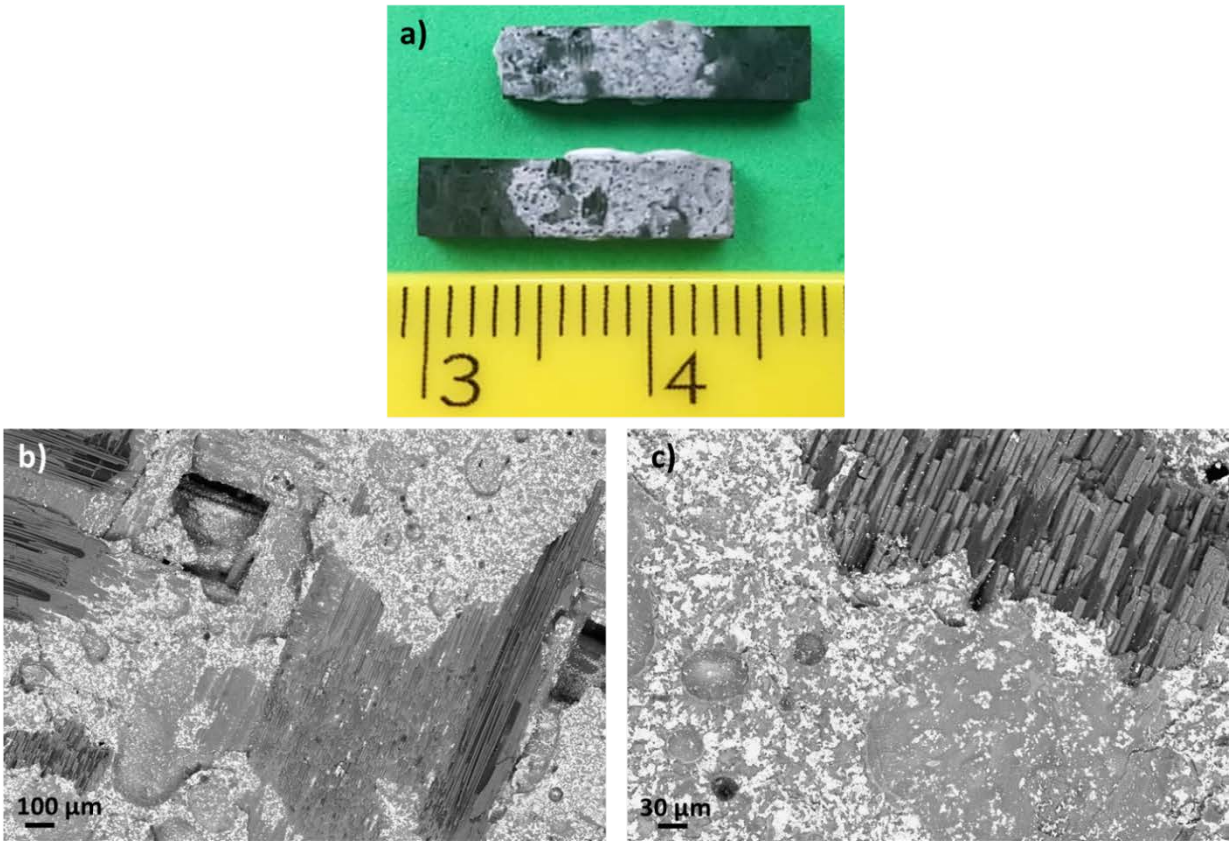

Figure 9. (a) Macrograph and (b, c) SEM micrographs (BSE) of the fracture surfaces after the SLO mechanical test on a glass-ceramic C/SiC joined sample.

Conclusions

This paper reported an interesting method to process an ytterbium disilicate based glass-ceramic material by reactive viscous flow sintering between a barium aluminium borosilicate glass matrix and ytterbium oxide to join C/SiC and SiC/SiC composites.

These findings have important implications for developing reliable and low cost glass-ceramic joining for CMCs. The results presented in this section are significant in at least two major respects:

-The joining process, on the basis of sintering and crystallization mechanism, is carried out without the use of pressure,

-The as-produced glass-ceramic system, with two different glassy phases, showed self-healing behaviour, thus opening the possibility to extend their performance where thermal cycles operating conditions are foreseen.

References

[1] P. Tatarko, S. Grasso, T.G. Saunders, V. Casalegno, M. Ferraris, M.J. Reece, Flash joining of CVD-SiC coated Cf/SiC composites with a Ti interlayer, J. Eur. Ceram. Soc. 37 (2017) 3841–3848. https://doi.org/10.1016/j.jeurceramsoc.2017.05.016.

[2] Y. Katoh, L.L. Snead, T. Cheng, C. Shih, W.D. Lewis, T. Koyanagi, T. Hinoki, C.H. Henager, M. Ferraris, Radiation-tolerant joining technologies for silicon carbide ceramics and composites, J. Nucl. Mater. 448 (2014) 497–511. https://doi.org/10.1016/j.jnucmat.2013.10.002.

[3] P. Tatarko, Z. Chlup, A. Mahajan, V. Casalegno, T.G. Saunders, I. Dlouh, M.J. Reece, High temperature properties of the monolithic CVD β-SiC materials joined with a pre-sintered MAX phase Ti3SiC2 interlayer via solid-state diffusion bonding, J. Eur. Ceram. Soc. 37 (2017) 1205–1216. https://doi.org/10.1016/j.jeurceramsoc.2016.11.006.

[4] M. Herrmann, S. Ahmad, W. Lippmann, H.-J. Seifert, A. Hurtado, Rare earth (RE: Nd, Dy, Ho, Y, Yb, and Sc) aluminosilicates for joining silicon carbide components, Int. J. Appl. Ceram. Technol. 14 (2017) 675–691. https://doi.org/10.1111/ijac.12692.

[5] H. Xiong, B. Chen, Y. Pan, H. Zhao, L. Ye, Joining of Cf/SiC composite with a Cu – Au – Pd – V brazing filler and interfacial reactions, J. Eur. Ceram. Soc. 34 (2014) 1481–1486. https://doi.org/10.1016/j.jeurceramsoc.2013.12.022.

[6] D.-H. Hyok, I.E. Reimanis, A review on the joining of SiC for high-temperature applications, J. Korean Ceram. Soc. 57 (2020) 246–270. https://doi.org/10.1007/s43207-020-00021-4.

[7] C. Jiménez, K. Mergia, M. Lagos, P. Yialouris, I. Agote, V. Liedtke, S. Messoloras, Y. Panayiotatos, E. Padovano, C. Badini, C. Wilhelmi, J. Barcena, Joining of ceramic matrix composites to high temperature ceramics for thermal protection systems, J. Eur. Ceram. Soc. 36 (2016) 443–449.

[8] X. Zhao, L. Duan, W. Liu, Y. Wang, Shear strength enhancement of SiC-coated 3D C/SiC composite joints with a Ni-Ti-Nb multi-interlayer by interfacial microstructure tailoring, J. Eur. Ceram. Soc. 39 (2019) 5473–5478. https://doi.org/10.1016/j.jeurceramsoc.2019.08.013.

[9] M. Patel, V. Singh, S. Singh, V.V. B. Prasad, Micro-structural evolution during diffusion bonding of C-SiC/C-SiC composite using Ti interlayer, Materials Characterization 135 (2018) 71–75

[10] P. Fitriani, H. Kwon, X. Zhou, D.H. Yoon, Joining of SiCf/SiC using a layered Ti3SiC2-SiCw and TiC gradient filler, J. Eur. Ceram. Soc. 40 (2020) 1043-1051, https://doi.org/10.1016/j.jeurceramsoc.2019.11.080

[11] M. B. Ruggles-Wrenn, T. M. Williams, Fatigue of a SiC/SiC ceramic composite with an ytterbium disilicate environmental barrier coating at elevated temperature, Int J Appl Ceram Technol. 2020, 00:1–9

[12] H. Zhao, B.T. Richards, C.G. Levi, H.N.G. Wadley, Molten silicate reactions with plasma sprayed ytterbium silicate coatings, Surf. Coat. Technol. 288 (2016) 151–162. https://doi.org/10.1016/j.surfcoat.2015.12.053.

[13] B.T. Richards, K.A. Young, F. De Francqueville, S. Sehr, M.R. Begley, H.N.G. Wadley, Response of ytterbium disilicate-silicon environmental barrier coatings to thermal cycling in water vapor, Acta Mater. 106 (2016) 1–14. https://doi.org/10.1016/j.actamat.2015.12.053.

[14] F. Smeacetto, M. Ferraris, M. Salvo, Multilayer coating with self-sealing properties for carbon–carbon composites, Carbon 41 (2003) 2105–2111

[15] C. Isola, M. Salvo, M. Ferraris, M.A. Montorsi, Joining of surface modified carbon/carbon composites using a barium-aluminum-boro-silicate glass, J. Eur. Ceram. Soc. 18 (1998) 1017–1024. https://doi.org/10.1016/S0955-2219(97)00203-3.

[16] ASTM D905-08 Standard Test Method for Strength Properties of Adhesive Bonds in Shear by Compression Loading, ASTM Int., West Conshohocken, PA USA (2013).

[17] F. Smeacetto, M. Salvo, M. Ferraris, Oxidation protective multilayer coatings for carbon–carbon composites, Carbon N. Y. 40 (2002) 583–587. https://doi.org/10.1016/S0008-6223(01)00151-8.

[18] M.J. Pascual, A. Durán, M.O. Prado, A new method for determining fixed viscosity points of glasses, Phys. Chem. Glas. 46 (2005) 512–520.

[19] A. Pavlik, S. V. Ushakov, A. Navrotsky, C.J. Benmore, R.J.K. Weber, Structure and thermal expansion of Lu2O3 and Yb2O3 up to the melting points, J. Nucl. Mater. 495 (2017) 385–391. https://doi.org/10.1016/j.jnucmat.2017.08.031.

[20] R.N. Singh, Sealing Technology for Solid Oxide Fuel Cells, Int. J. Appl. Ceram. Technol. 4 (2007) 134–144. https://doi.org/10.1002/9783527650248.ch11.

Captions

Figure 1. (a) Hot stage microscope analyses of the SABB glass (curve a) and SABB+Yb2O3 mixture 2:1 wt. (curve b), both recorded at 10 °C/min. (b) Log η vs Temperature curve for the SABB glass (curve a) and SABB+Yb2O3 mixture (2:1 by weight) (curve b), obtained by fitting the characteristic fixed viscosity points and related temperatures (Tfs, Tms, TD, Tsp, Ths) reported in Table I.

Figure 2. XRD pattern of the mixture of SABB glass and ytterbia mixture (2:1 by weight) after the heat treatment at 1200°C for 1 hour; $Yb_2Si_2O_7$ indexed by the PDF card n. 00-025-1345; Yb_2O_3 indexed by the PDF card n. 01-074-1981.

Figure 3. SEM images of the cross-section of (a, b) a glass-ceramic joined SiC/SiC sample and (c,d) a glass-ceramic joined C/SiC sample.

Figure 4. SEM, Ba elemental map and EDS analyses of the ytterbium disilicate based glass-ceramic from the joining area

Figure 5. Schematic of the glass-ceramic system microstructure: (a) before and (b) after crack formation, (c) self- healing during reheating at a temperature higher than the softening temperature (T soft) of the Ba-rich glassy phase and lower than the deformation temperature (DT) of the whole glass-ceramic system.

Figure 6. Optical images of the indents made at 0.5 kg (HV0.5) (a) before, (b) after annealing at 1000°C/30 min, and (c) after annealing at 1150°C/20min; 1 kg (HV1) (d) before, (e) after annealing at 1000°C/30 min, and (f) after annealing at 1150°C/20min.

Figure 7. 3D images (confocal microscopy) of the indents made at 1 kg (HV1) (a) before, (b) after annealing at 1000°C/30 min, and (c) after annealing at 1150°C/20 min.

Figure 8. (a, b) Macrographs of a glass-ceramic joined SiC/SiC with a joining area of ~ 42 mm^2 (the red circle indicates the crack formation in the composite) and (c, d) SEM micrographs (BSE) of the fracture surfaces after the SLO mechanical test on a glass-ceramic joined SiC/SiC with a joining area ~ 20 mm^2

Figure 9. (a) Macrograph and (b, c) SEM micrographs (BSE) of the fracture surfaces after the SLO mechanical test on a glass-ceramic C/SiC joined sample.

Table I. Characteristic temperatures at fixed viscosity values for the SABB glass and the SABB+Yb2O3 mixture (2:1 by weight). Viscosity values from [18].